ELSEVIER

Thermochimica Acta 303 (1997) 69–76

thermochimica acta

Kinetics and mechanism of the isothermal dehydration of zinc acetate dihydrate

Nobuyoshi Koga*, Haruhiko Tanaka

Chemistry Laboratory, Faculty of School Education, Hiroshima University, 1-1-1 Kagamiyama, Higashi-Hiroshima 739, Japan

Received 6 March 1997; received in revised form 27 March 1997; accepted 24 June 1997

Abstract

The overall kinetics of the thermal dehydration of zinc acetate dihydrate was investigated by means of isothermal mass-change measurements, complemented by microscopic observations of the reaction geometry and morphological change during the reaction. Under isothermal conditions, the compound loses its water of crystallization in a well-defined single step; $Zn(CH_3COO)_2 \cdot 2H_2O \rightarrow Zn(CH_3COO)_2 + 2H_2O$. The microscopic observations for the single crystals confirm that the reaction initiates at the edge surfaces of the hexagonal thin plate by nucleation and growth processes, consequently forming the reaction interface which advances inward, toward the center of the hexagon. The kinetic results obtained from the thermoanalytical measurements indicated agreement to the first-order law, in spite of the two-dimensional shrinkage of the reaction interface. This discrepancy is discussed in connection with the interactions of the elementary nucleation and growth processes at the reaction interfaces with the self-generated water vapor. The overall kinetic behavior of the crushed crystals of different particle-size fractions, under various atmospheric conditions, was investigated. The apparent kinetic results varied systematically with the sample and atmospheric conditions, accompanied by changes of the roles of surface reaction, diffusion of evolved water vapor from the reaction interface and gross diffusion of water vapor through the assemblage of sample particles. © 1997 Elsevier Science B.V.

Keywords: Isothermal dehydration; Kinetics; Microscopy; Reaction interface; Thermal analysis; Zinc acetate dihydrate

1. Introduction

Kinetic and mechanistic studies of the dehydration of crystalline hydrates have contributed very notably toward the provision of a theoretical foundation for the understanding of solid-state reactions [1]. The kinetic models have been established fundamentally on the basis of the microscopic measurements of the reaction geometry and the kinetics of the reaction interface advancement [2,3], because many such rate processes are characterized by the existence of the specialized zone of locally enhanced reactivity at the reactant/product contact. Thermoanalytical (TA) measurements have been widely used for obtaining kinetic data [4]. Some difficulties have been found in providing a satisfactory kinetic description by comparison of macroscopically averaged TA data and the mathematically simplified physico-geometric models derived originally from the microscopically centered observations [5–7]. This seems to be due to the complexity of the kinetic behavior of the reaction interface advancement, making it difficult to interpret the overall kinetics from physico-chemical points of view.

*Corresponding author. Tel.: 81 824 24 7093; fax: 81 824 22 7105; e-mail: nkoga@dean.sed.hiroshima-u.ac.jp

PII S0040-6031(97)00264-5

The experimental conditions applied for TA measurements influence the interactions of the elementary processes at the reaction interfaces, producing different overall kinetic behavior depending on the experimental conditions [8,9]. The degree of coordination between the kinetic information from TA measurements and the physico-geometric models expected from the apparent reaction geometry is also affected by the experimental conditions. It must be noted that the actual reaction conditions deviate from the ideal by the additional factors produced by the reaction itself, e.g. self-cooling and/or -heating, partial pressure of evolved gas, and so on [10–13]. The effect of such self-generated conditions on the TA curves and/or kinetics also depends on the experimental conditions applied. For instance, with changing sample mass and heating rate the overall kinetics measured for the thermal decomposition process vary, being affected by mass- and heat-transfer phenomena [14].

It is expected that systematic investigation of the influence of the experimental conditions on the overall kinetics will lead to an understanding of such interactions in elementary processes. In the present study, the overall kinetics of the thermal dehydration of single-crystal zinc acetate dihydrate was investigated by means of isothermal mass-change measurements, complemented by microscopic observations of the reaction geometry and morphologies of reaction interfaces during the reaction. The crushed crystals were also subjected to kinetic study in order to evaluate the effects of particle size and the atmosphere. The kinetic results obtained for the dehydration under such different conditions are systematically compared. The changes in the overall kinetics are interpreted in connection with the interactions in elementary processes, suggesting possible variations in the kinetics and mechanisms of advance of the reaction interface.

2. Experimental

2.1. Zinc acetate dihydrate

Reagent-grade zinc acetate dihydrate (Katayama Chem.) was dissolved in water, and single crystals in the form of flat hexagonal plates were obtained by slow evaporation at ambient temperature from the aqueous solution, to which a small amount of acetic acid was added. Crushed crystals were obtained by grinding the single crystals in a pestle and mortar. After washing with 50%-ethanol, the crushed crystals were sieved to various particle-size fractions. The sample was identified by means of powder X-ray diffractometry, FTIR spectroscopy and thermogravimetry (TG), and stored for more than two weeks before carrying out kinetic measurements to avoid a possible ageing effect.

2.2. Kinetic measurements

Nearly 15.0 mg of reactant sample, single crystal or crushed crystals, were weighed onto a platinum crucible of 5 mm diameter and 2.5 mm height. Isothermal mass-change traces were recorded at various temperatures using a TG instrument (Shimadzu TGA-50) in static air or in an atmosphere of flowing N_2. The sample temperature was controlled to maintain the predetermined temperature within ± 1 K during the course of reaction, after heating from room temperature at a rate of 20 K min^{-1}. A buoyancy correction was performed for the mass-change traces using data from blank measurements. Derivative curves were obtained by numerical differentiation of the corrected mass-change traces.

2.3. Microscopic observations

Textural changes on typical surfaces, during isothermal dehydration of single crystals under conditions identical with the TA runs, were observed and photographed, using a reflection microscope with a programmable hot-stage (Linkam TH600). Observation of the textural changes at reaction interfaces was performed by preparing thin sections of partially dehydrated single crystals according to a technique described elsewhere [3,8]. The thin sections were observed and photographed under polarized light with the help of a microscope.

3. Results and discussion

3.1. Single crystals

3.1.1. Conventional kinetic analyses

Isothermal kinetic measurements were made for the dehydration of single crystals of $Zn(CH_3COO)_2 \cdot 2H_2O$

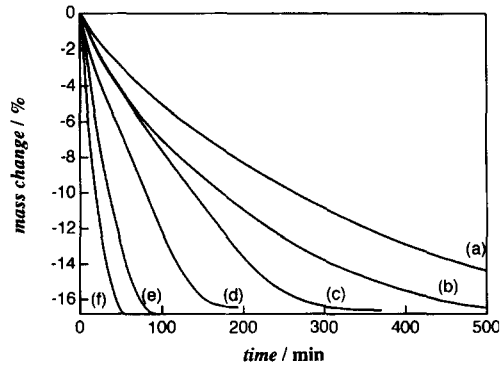

Fig. 1. Typical mass-change traces for the isothermal dehydration of single crystals in flowing N_2 (30 ml min^{-1}) at various temperatures: (a) 337; (b) 339; (c) 343; (d) 344; (e) 347; and (f) 357 K.

between 333 and 361 K. Fig. 1 shows typical mass-change traces under flowing N_2 at a rate of 30 ml min^{-1} at various temperatures. The sample was dehydrated quantitatively to anhydrous salt with smooth mass-loss traces;

$$Zn(CH_3COO)_2 \cdot 2H_2O \rightarrow Zn(CH_3COO)_2 + 2H_2O.$$

The overall behavior is predominantly deceleratory without any distinguishable induction period.

For the kinetic analysis, the following general kinetic equation was employed:

$$\frac{d\alpha}{dt} = A \exp\left(-\frac{E}{RT}\right) f(\alpha) \quad (1)$$

where α and $f(\alpha)$ are the fractional reaction and kinetic model function in the differential form [1–7], respectively. The other symbols represent their standard meanings. For the ideal kinetic process, straight lines with slopes of $-E/R$ are obtained from plots of ln $(d\alpha/dt)$ vs. T^{-1} at given values of α [15]. Fairly good linearity was obtained for the single crystals at various values of α ($0.04 \leq \alpha \leq 0.93$), with the correlation coefficients of linear regression analyses better than -0.98. The dependence of the apparent activation energy E on α for the isothermal dehydration of single crystals is shown in Fig. 2. The apparent E values increase with α in the range of $\alpha \leq 0.3$ and remain constant with the mean value of 165.4 ± 5.0 kJ mol^{-1} in the range $\alpha \geq 0.3$. The variation of the apparent E in the range $\alpha \leq 0.3$ can be interpreted as due to a change in the self-generated water vapor pressure at the reaction interface. This will be discussed later in connection with the effects of particle size and atmosphere on the kinetics of isothermal dehydration of crushed crystals. The constant E in the range $\alpha \geq 0.3$ satisfies the preliminary restriction of Eq. (1) and the rate process in the restricted range $0.3 \leq \alpha \leq 0.9$ was subjected to further kinetic analysis.

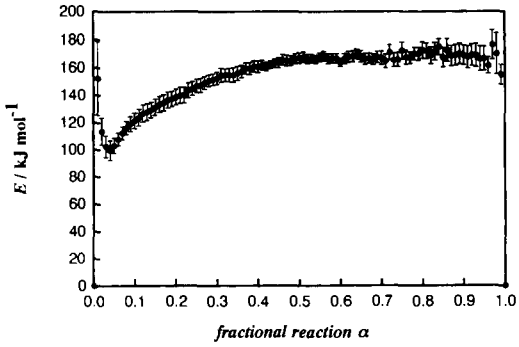

Fig. 2. The dependence of the apparent E values on α for the isothermal dehydration of single crystals.

Using the pre-determined E value, the rate data obtained from the respective TA runs were generalized by extrapolating these to infinite temperature [16], according to the following equation:

$$\frac{d\alpha}{d\theta} = \frac{d\alpha}{dt} \exp\left(\frac{E}{RT}\right) \quad \text{with}$$

$$\theta = \int_0^t \exp\left(-\frac{E}{RT}\right) dt \quad (2)$$

where θ is the generalized time proposed by Ozawa [17]. Fig. 3 shows a plot of $d\alpha/d\theta$ against α for the thermal dehydration of single crystals within the restricted range $0.3 \leq \alpha \leq 0.9$. The error bars indicate the standard deviations among the kinetic curves at different temperatures. The value of $d\alpha/d\theta$ decreases monotonously with α. At infinite temperature, the kinetic equation is expressed by [6,16,17]

$$\frac{d\alpha}{d\theta} = Af(\alpha) \quad (3)$$

The monotonous decrease in $d\alpha/d\theta$ with α indicates the possible agreement to the first-order F_1 law;

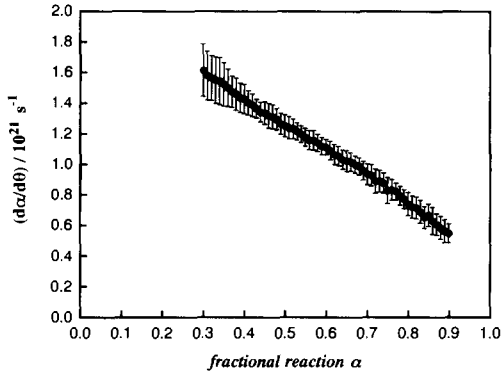

Fig. 3. A plot of $d\alpha/d\theta$ against α for the isothermal dehydration of single crystals within the restricted range $0.3 \leq \alpha \leq 0.9$.

Fig. 4. A typical microscopic view of an edge surface of a hexagonal thin-plate single crystal, at the beginning of isothermal dehydration.

$f(\alpha) = (1 - \alpha)$, with a correlation coefficient of the linear regression analyses of $d\alpha/d\theta$ vs. $(1 - \alpha)$ plot better than 0.999. The apparent preexponential factor A obtained from the slope was $(1.75 \pm 0.16) \times 10^{21}$ s^{-1}. The apparent kinetic results for the isothermal dehydration of the single crystals are summarized in Table 1.

3.1.2. Microscopic observation

Through the hot-stage microscopic observation, it was recognized that the dehydration initiates at the edge surface of single crystals in the form of hexagonal thin plates. Fig. 4 shows a typical microscopic view of an edge surface at the very beginning of the reaction. Dehydration products are recognized at sites parallel to the most developed surface (010). The reactivity of the sites on the edge surfaces can be explained by the structure of the single crystals, in which the single crystals assume the form of thin plates which are stacked together to form prisms, with the prism surfaces (100) and (001) [18]. Fig. 5(a) represents the polarizing microscopic view of the internal (010) surfaces of thin sections of partially dehydrated single crystals. It is seen that the reaction proceeds according to the advance of the reaction interface from the edge surfaces to the center of the hexagon. Because reaction at the (010) surface is not marked at this stage, the reaction geometry is identified as the contracting-area type and, thus, agreement to the two-dimensional phase boundary control law, R_2, is expected if the linear rate of reaction interface movement is constant during the course of the reaction.

This assumption is not in line with the results of the kinetic analysis described above. The change in the apparent values of E during the course of reaction indicates the change in the overall rate of interface advance (see Fig. 2). Fig. 5(b) shows a typical texture of the reaction interface observed under polarized light. The reaction interface is not planar and is different from the simple reactant–product contact assumed in the conventional physico-geometric kinetic model functions. The product layer is composed of needle-like crystallites oriented very approximately in the direction of advancement of the reaction interface. Accordingly, nucleation at the reaction interface and one-dimensional growth of the nuclei

Table 1
The apparent kinetic results obtained for the isothermal dehydration of $Zn(CH_3COO)_2 \cdot 2H_2O$ under flowing N_2 at a rate of 30 ml min^{-1}

Particle size	Range of α	E/ (kJ mol^{-1})	$f(\alpha)$	Exponent	A/s^{-1}	γ [a]
Single crystal	$0.30 \leq \alpha \leq 0.90$	165.4±5.0	$1 - \alpha$	—	1.75×20^{21}	0.9993
−24 + 32 Mesh	$0.10 \leq \alpha \leq 0.90$	101.3±3.0	$n(1 - \alpha)^{1-1/n}$	$n = 3.0$	5.53×10^{11}	0.9998
−170 + 200 Mesh	$0.15 \leq \alpha \leq 0.70$	75.1±2.9	$m(1 - \alpha)[-\ln(1 - \alpha)]^{1-1/m}$	$m = 1.2$	7.16×10^{8}	0.9991

[a] Correlation coefficient of the linear regression analysis of the $d\alpha/d\theta$ vs. $f(\alpha)$ plot.

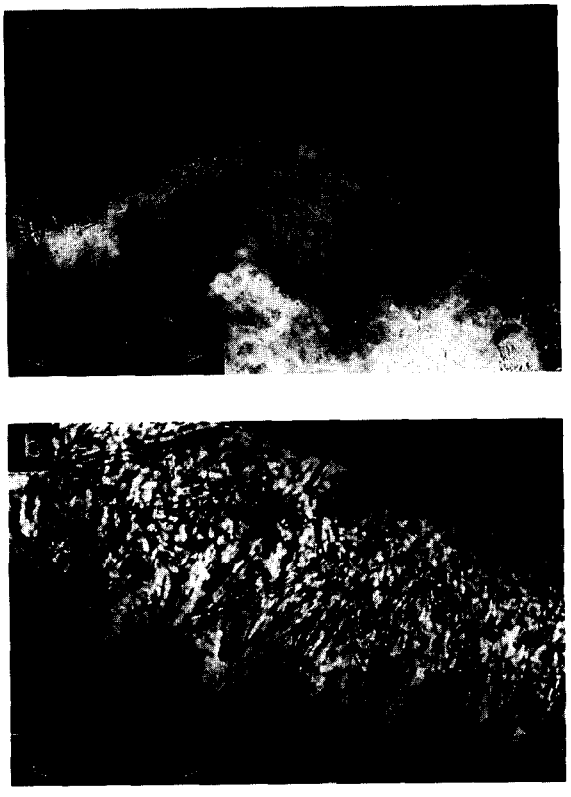

Fig. 5. Typical polarizing microscopic views of the internal (010) surfaces of partially dehydrated single crystals.

are identified as one of the characteristics of the present reaction. The destruction of the crystal structure, including the breaking of bonds and ionic movement, also plays an important role as is expected from the irregularity in the shape of the reactant–product contact. These elementary processes take place under a self-generated water vapor pressure, and the diffusional removal of water vapor from the reaction interface influences the overall kinetics of the dehydration.

3.2. Crushed crystals

3.2.1. Effect of particle size

Fig. 6 shows the kinetic behavior of isothermal dehydration of crushed crystals in flowing N_2 (30 ml min^{-1}) at 333 K, as plots of $d\alpha/dt$ vs. α. The rate of dehydration and the shape of the $d\alpha/dt$ vs. α plot change with different particle size fractions. Fig. 7 represents the dependence of the apparent E on α obtained from the slopes of the ln $(d\alpha/dt)$ vs. T^{-1}

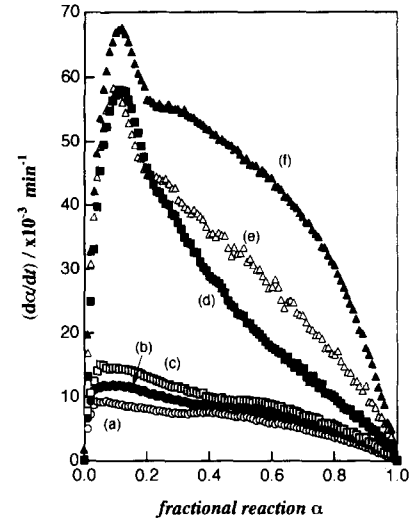

Fig. 6. Effect of particle size on the rate of isothermal dehydration of crushed crystals in flowing N_2 (30 ml min^{-1}) at 333 K: (a) −16 + 24; (b) −24 + 32; (c) −32 + 48; (d) −48 + 100; (e) −100 + 170; and (f) −170 + 200 mesh sieve fractions.

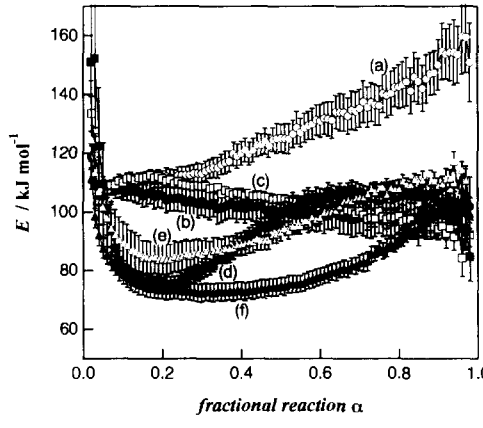

Fig. 7. Comparison of the dependence of the apparent E values on α for the isothermal dehydration of crushed crystals of various fractions of particle size in flowing N_2 (30 ml min^{-1}): (a) −16 + 24; (b) −24 + 32; (c) −32 + 48; (d) −48 + 100; (e) −100 + 170; and (f) −170 + 200 mesh sieve fractions.

plots for the crushed crystals of different particle-size fractions. It is worth noting that the dependence of apparent E on α among the different particle-size fractions changes very systematically. Four types of α dependences were recognized within the particle-size fractions examined. The E values of the −16 + 24 mesh fraction increased gradually with α

from ca. 110 to 160 kJ mol^{-1}. Nearly constant values of E were obtained, irrespective of α, for the fractions of $-24+32$ and $-32+48$ meshes. The mean values of E for the $-24+32$ and $-32+48$ meshes in the range of $0.1 \leq \alpha \leq 0.9$ were 101.3 ± 3.0 and 103.1 ± 4.9 kJ mol^{-1}, respectively. Two ranges of constant E were observed for $-48+100$ and $-100+170$ meshes, in which the lower value of E of ca. 80 kJ mol^{-1} in the range of $0.1 \leq \alpha \leq 0.3$ changes to the higher E value of ca. 100 kJ mol^{-1} in the range of $\alpha \geq 0.5$. For the $-170+200$ mesh sample, the E value of ca. 80 kJ mol^{-1} in the early stage of the reaction remains constant over a wider range of α than those for the $-48+100$ and $-100+170$ meshes, followed by a gradual increase to ca. 110 kJ mol^{-1} in the range $\alpha \geq 0.6$.

The rate processes for the $-24+32$ and $-170+200$ mesh samples in the restricted ranges of $0.1 \leq \alpha \leq 0.9$ and $0.15 \leq \alpha \leq 0.7$, respectively, were subjected to further kinetic characterization. For these processes, the mean values of apparent E in the respective ranges of α were 101.3 ± 3.0 and 75.1 ± 2.9 kJ mol^{-1}, respectively. Fig. 8 shows the rate behavior extrapolated to infinite temperature as the plot of $d\alpha/d\theta$ vs. α. Both the curves are characterized predominantly as deceleratory and convex. The major difference between the plots is seen in the range $\alpha \leq 0.4$. The plot for the $-170+200$ mesh sample indicates a maximum at around $\alpha = 0.1$, which favors agreement with the Avrami–Erofeev laws, A_m. The rate processes for the $-24+32$ and $-170+200$ mesh fractions, within the respective restricted ranges of α, were satisfactorily described by the contracting-volume $R_{3.0}$ and $A_{1.2}$ laws, respectively. The kinetic results obtained for the crushed crystals are summarized in Table 1.

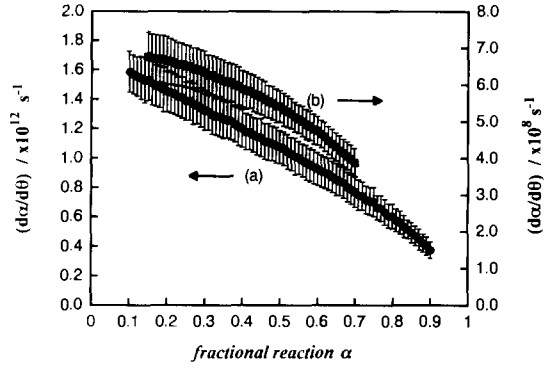

Fig. 8. Plots of $d\alpha/d\theta$ vs. α for the isothermal dehydration of crushed crystals of (a) $-24+32$ and (b) $-170+200$ mesh sieve fractions in the ranges of $0.1 \leq \alpha \leq 0.9$ and $0.15 \leq \alpha \leq 0.7$, respectively.

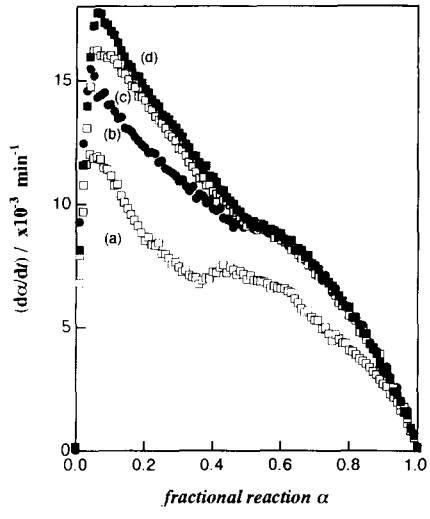

Fig. 9. Effect of the flow rate of N_2 on the rate of the isothermal dehydration of crushed crystals ($-16+24$ mesh) at 337 K: (a) 0; (b) 15; (c) 30; and (d) 45 ml min^{-1}.

3.2.2. *Effect of atmosphere*

For the fractions of $-16+24$ and $-100+170$ meshes, the effect of atmosphere on the kinetics was examined to investigate the role of gross diffusion of the evolved water vapor through the matrix of the particle assemblage. Fig. 9 shows the effect of N_2 flow on the isothermal rate behavior at 337 K of the $-16+24$ mesh fraction as plots of $d\alpha/dt$ vs. α. Apparently, the dehydration kinetics depends on the rate of N_2 flow. The reaction under static air proceeds at a lower transformation rate during the course of reaction. The transformation rate in the range $\alpha \leq 0.5$ increases with the rate of N_2 flow. In the range $\alpha \geq 0.5$, the rate of dehydration is not markedly affected by the rate of N_2 flow, suggesting the significance of the diffusional removal of water vapor through the solid–product layer at this stage. For the sample of $-100+170$ mesh fraction, the increase in reaction rate with the flow rate of N_2 was observed during the course of reaction. The difference in the effect of the flow rate between the two different particle-size fractions is thought to be experimental

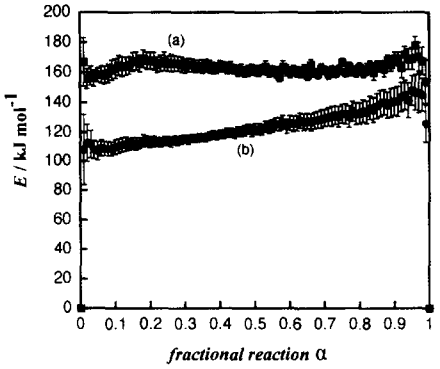

Fig. 10. The dependence of the apparent E on α values for the isothermal dehydration of crushed crystals ($-16 + 24$ mesh) under (a) static air and (b) flowing N_2 at a rate of 45 ml min^{-1}.

evidence that the effect of gross diffusion of the water vapor on the overall kinetics is more predominant for the sample of smaller particle sizes. In contrast, it is seen from the rate behavior in the range $\alpha \geq 0.5$ for $-16 + 24$ mesh (see Fig. 9) that diffusion of the water vapor evolved at the reaction interface through the solid–product layer plays an important role in the overall kinetics for the sample of larger particle sizes.

Fig. 10 represents the dependence of the apparent E values on α for crushed crystals of $-16 + 24$ mesh under static air and under flowing N_2 at a rate of 45 ml min^{-1}. Under static air, the apparent E values remain constant with a mean value of 160.3 ± 1.2 kJ mol^{-1} ($0.1 \leq \alpha \leq 0.9$). This value is in good agreement with that of single crystals in the range $\alpha \geq 0.3$. In flowing N_2, the apparent value of E increased gradually from ca. 100 to 160 kJ mol^{-1} as the reaction advances. The rate behavior under static air, extrapolated to infinite temperature, was characterized by a monotonous decrease in the value of $d\alpha/d\theta$ with α, indicating possible agreement with the first-order equation, as is the case of the single crystals in the range $\alpha \geq 0.3$. The correspondence in the kinetic results for the single crystals in flowing N_2 and crushed crystals ($-16 + 24$ mesh) in static air possibly indicates the significant role of diffusional removal of the self-generated water vapor through the solid–product layer and/or through the matrix of the sample particles. This is also supported by the gradual increase in the E values with α for the crushed crystals ($-16 + 24$ mesh) in flowing N_2, to ca. 160 kJ mol^{-1}. Under such reaction conditions, the effect of the reverse reaction has to be taken into account for a physico-chemical interpretation.

3.3. Kinetic interpretation

The overall kinetic behavior of the isothermal dehydration of the single crystals and crushed crystals can be understood by following the systematic variation of the apparent E values with the sample and atmospheric conditions. The rate process with the E value of ca. 160 kJ mol^{-1} was observed for single crystals in flowing N_2 and crushed crystals ($-16 + 24$ mesh) in static air. In this case, the reactions take place under conditions of relatively high water vapor pressure. Although two-dimensional shrinkage of the reaction interface was evident from microscopic observations, the kinetic behavior evaluated from the TA curves indicated the apparent agreement with the first-order law. For this process, the physico-geometry of the kinetic model function evaluated does not correspond to the actual reaction geometry. The apparent agreement to the first-order law can be interpreted by assuming that diffusion of the evolved water vapor through the assemblage of finely dispersed product crystallites is the rate limiting step [19]. Similar behavior has been observed for the thermal dehydration of several crystalline hydrates [8,9,20].

For the isothermal dehydration of crushed crystals of sieve fractions $-24 + 32$ and $-32 + 48$ meshes in flowing N_2, the E value of ca. 100 kJ mol^{-1} was obtained over the entire course of the reaction. The process was well characterized by the contracting-geometry-type law, $R_{3.0}$. Taking into account the effect of grinding on crushed crystals, it seems that the $R_{3.0}$ law evaluated from kinetic analysis shows fairly good geometric correspondence to the actual reaction geometry. Accordingly, the evaluated E value, ca. 100 kJ mol^{-1}, can be identified as the apparent activation energy for advancement of the reaction interface.

On decreasing the particle size to $-170 + 200$ mesh, the early stage of the reaction is characterized by an E value of ca. 80 kJ mol^{-1}. It is generally accepted that the role of the surface reaction increases with decreasing particle size. The Avrami–Erofeev-type law, $A_{1.2}$, was determined as the most appropriate kinetic model function. This implies that the process defined by the E value of 80 kJ mol^{-1} is regulated by nucleation and

growth processes at the surfaces. Such dependence of the overall kinetics on surface reaction is also seen in the surface-induced crystallization in glasses [21]. With decreasing size of the glass particle, the overall kinetics of crystallization tends to obey the F_1 law [22].

In conclusion, the dehydration reaction essentially consists of formation of nuclei of the anhydrous salt and the one-dimensional growth of the nuclei, resulting in a two-dimensional advance of the reaction interface toward the center of the hexagonal single crystal and/or crushed crystals. These kinetic processes are apparently influenced by self-generated water vapor. As the result of the interactions of these kinetic processes, the apparent rate-controlling step in the overall kinetics changes with the experimental conditions. Within the conditions of sample and atmosphere examined in the present study, the overall kinetics of the isothermal dehydration are well described by three distinguishable rate behaviors with characteristic values of E as follows:

1. a surface reaction induced mechanism observed for the smaller particle sizes;
2. a phase boundary reaction controlled mechanism for the medium-sized particles under flowing N_2; and
3. a nucleation and growth mechanism at the reaction interface, affected by the diffusional removal of the evolved water vapor for single crystals and larger particle sizes.

It is worth noting that the overall kinetic behavior varies with the applied sample and atmospheric conditions in a systematic way. This seems to result from the gradual variation in the overall rate-limiting step caused by the influence of the experimental conditions on the complicated interactions and/or competitions of the elementary steps at the reaction interface.

References

[1] M.E. Brown, D. Dollimore and A.K. Galwey, Reactions in the Solid State, Elsevier, Amsterdam, 1980.
[2] S.F. Hulbert, J. Br. Ceram. Soc., 6 (1969) 11.
[3] H. Tanaka, N. Koga and A.K. Galwey, J. Chem. Educ., 72 (1995) 251.
[4] J. Sestak, Thermophysical Properties of Solids, Elsevier, Amsterdam, 1984.
[5] A.K. Galwey, Thermochim. Acta, 96 (1985) 259.
[6] N. Koga, J. Malek, J. Sestak and H. Tanaka, Netsu Sokutei (Calor. Therm. Anal.), 20 (1993) 210.
[7] N. Koga, J. Therm. Anal. (Proc. 11th ICTAC), 49 (1997) 45.
[8] N. Koga and H. Tanaka, J. Phys. Chem., 93 (1989) 7793; 98 (1994) 10521; Solid State Ionics, 44 (1990) 1.
[9] H. Tanaka, N. Koga and J. Sestak, Thermochim. Acta, 203 (1992) 203.
[10] J. Sestak, Talanta, 13 (1966) 567.
[11] J. Rouquerol, J. Therm. Anal., 5 (1973) 203.
[12] H. Tanaka and N. Koga, J. Therm. Anal., 36 (1990) 2601.
[13] J.P. Czarnecki, N. Koga, V. Sestakova and J. Sestak, J. Therm. Anal., 38 (1992) 575.
[14] P.K. Gallagher and D.W. Johnson Jr., Thermochim. Acta, 6 (1973) 67.
[15] H.L. Friedman, J. Polym. Sci., Part C, 6 (1964) 183.
[16] N. Koga, Thermochim. Acta, 258 (1995) 145.
[17] T. Ozawa, Bull. Chem. Soc. Jpn., 38 (1965) 1881; J. Therm. Anal., 2 (1970) 301; Thermochim. Acta, 100 (1986) 109; J. Therm. Anal., 31 (1986) 547.
[18] J.N. van Niekerk, F.R.D. Schoening and J.H. Talbot, Acta Cryst., 6 (1953) 720.
[19] V.B. Okhotonikov, React. Kinet. Catal. Lett., 38 (1989) 369.
[20] H. Tanaka and N. Koga, J. Phys. Chem., 92 (1988) 7023.
[21] N. Koga and J. Sestak, Bol. Soc. Esp. Ceram. Vidr., 31 (1992) 185.
[22] N. Koga, J. Sestak and Z. Strnad, Thermochim. Acta, 203 (1992) 361.